Shaking table test of a full scale stone masonry building with stiffened floor and roof diaphragms

G. Magenes & A. Penna
University of Pavia and European Centre for Training and Research in Earthquake Engineering (EUCENTRE), Pavia, Italy

M. Rota
EUCENTRE, Pavia, Italy

A. Galasco
University of Pavia, Pavia, Italy

I. Senaldi
ROSE School, IUSS, Pavia, Italy

SUMMARY
Shaking table tests on three full-scale, two-storey prototype buildings in undressed double-leaf stone masonry were performed as part of the extensive experimental program carried out at EUCENTRE, for the evaluation and reduction of the seismic vulnerability of stone masonry structures. The three buildings were designed with the same geometrical configuration and construction materials but the last two were strengthened to improve the connections of floor and roof diaphragms with walls and to achieve different levels of in-plane diaphragm stiffness by using traditional and innovative solutions. The paper concentrates on the third building tested and, in particular, it describes the characteristics of the strengthening interventions and presents the results obtained during the dynamic tests, illustrating the response of the structure, the damage mechanism and its evolution during the tests.

Keywords: Shaking table test, stone masonry, full scale, strengthening strategies, stiffening of diaphragms

1. INTRODUCTION

The high vulnerability of existing unreinforced masonry structures and the effectiveness of strengthening interventions are topics of great interest in the construction world, as also recognised by several post-earthquake damage surveys. In particular, stone masonry has proved to be one of the most vulnerable typologies but, although significant numerical and experimental research has been carried out in the past (e.g. Tomazevic *et al*, 1992, Benedetti *et al*., 1998, Dolce *et al*., 2008, Mazzon *et al*., 2009), a shake-table testing campaign on full-scale building specimens had not been carried out to present.

A comprehensive experimental program on the assessment of the seismic performance of double-leaf stone masonry buildings has been undertaken at EUCENTRE in the last years. As part of the testing campaign, preliminary characterization tests were carried out, including vertical and diagonal compression tests on wallettes (Magenes *et al*., 2010a), in-plane cyclic tests on large masonry piers (Magenes *et al*., 2010b) and spandrels (Graziotti *et al*., 2012). Shake table tests were then carried out on three full-scale, two-storey buildings, all designed with the same geometrical configuration and construction materials but with different levels of in-plane stiffness of floor and roof diaphragms. This paper concentrates in particular on the third building tested, as the first prototype has been already described in Magenes *et al*. (2010c) while the second building is presented in Magenes *et al*. (2012).

2. THIRD STONE MASONRY PROTOTYPE BUILDING

2.1 Design and construction of the third prototype building

2.1.1. Geometry of Building 3

The geometry of the third prototype building was designed to reproduce at full scale the basic characteristics of old stone masonry structures, although limited in size and weight by the driving capacity of the shaking table and of the transportation system. The building had also to be asymmetric to enhance the role of the floor and roof in-plane stiffness. Fig. 1 represents the geometry of the third prototype, designed as a single-room, two storey building with pitched roof. The longitudinal walls, namely the East and West façades, are oriented in the direction of the shaking table motion. The geometry is similar to that of the first building tested in the experimental campaign (Building 1), described in Magenes *et al*. (2010a). The third building prototype represents the original structure of Building 1, on which specific interventions were applied to stiffen significantly the wooden floor and roof diaphragms and to improve their connections with the masonry walls.

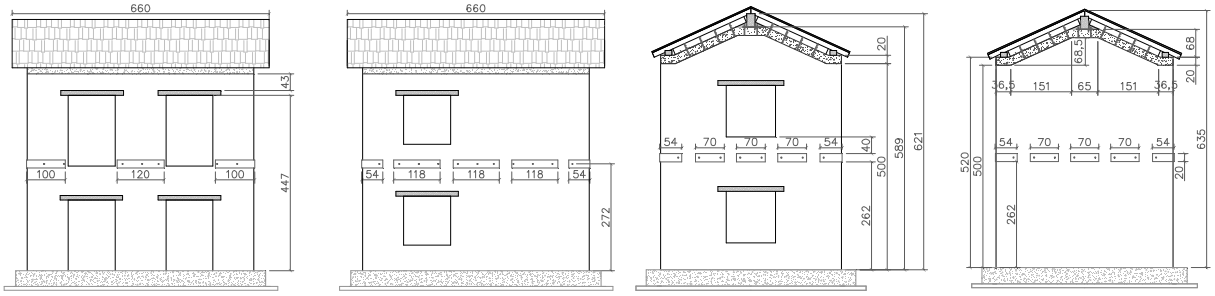

Figure 1. Elevation views of the walls of the building specimen with indication of dimensions (in cm). From left: West, East, North and South façades.

2.1.2. Material properties and masonry characterization tests

All the specimens included in the experimental program were made of double-leaf stone masonry, without through stones (apart from corners and vicinity of openings, where some through stones were present as observed in most existing buildings), with a nominal thickness of 32 cm. The two leaves of undressed stones were simply built one close to the other, with some smaller stones and mortar used to fill the irregular gaps in between. Table 2.1 summarises the mechanical properties determined from simple compression and diagonal compression tests, as described in detail in Magenes *et al*. (2010b).

Table 2.1. Summary of masonry mechanical properties after characterization tests in MPa (6 specimens per test)

	Compressive strength (f_m)	Young's modulus (E)	Tensile strength for diagonal shear (f_t)	Shear modulus (G)
Mean	3.28	2537	0.138	841
St. Dev.	0.26	378.7	0.030	141.5
c.o.v.	8%	14.9%	22.1%	16.8%

2.2 Details of the strengthening interventions for Building 3

The strengthening interventions were designed to prevent the activation of out-of-plane failure modes and to ensure a global type of response of the structure under seismic excitation. Traditional and innovative solutions were conceived to enhance the connections between orthogonal walls and between walls and floors/roofs and the in-plane diaphragm stiffness. The choice of the type of strengthening was also based on the results of the experimental campaign carried out at the University of Trento for different floors typologies (Piazza *et al*., 2008) that demonstrated the effectiveness of diaphragms in increasing the in-plane stiffness, obtained through the addition of wood panels or by casting in place a concrete slab, appropriately connected to the existing wooden floor.

Simulating an intervention where the roof structure can be temporarily removed, a reinforced concrete ring beam, 20 cm high and 32 cm wide (as the wall below), was cast at the roof level, on top of the perimeter façades (Fig. 2, left). The reinforcement consisted in 4ϕ16 longitudinal bars and ϕ8 stirrups at a spacing of 20 cm, coherently with the prescriptions of the Italian Building Code (NTC08, 2008).

Figure 2. Detail of the reinforcement of the joint at the base of the gable wall (left). Operation of drilling the timber spreader beam and the concrete ring beam (right)

The original timber roof structure of the unstrengthened building included one 20cm x 32 cm ridge beam, two segmented 32cm x 12cm spreader beams on top of the longitudinal walls and 8cm x 12 cm purlins every 50 cm forming the two pitches with 30 mm thick planks.
The strengthening of the roof envisaged the improvement of the connection of the ridge beam with the gable walls, which consisted of a steel shoe doweled to the concrete ring beam and bolted to the ridge beam. Timber spreader beams were also doweled to the r.c. ring beam all along the perimeter, by means of connecting steel bars chemically anchored by epoxy resin. Any discontinuity between the timber spreader beam and the ring beam was smoothed by the insertion of a plaster layer to create a continuous contact. The 8 cm x 12 cm joists were reshaped to create a horizontal seat on the ridge beam and on the longitudinal spreader beams. Steel connecting elements were inserted at the top of the ridge beam, at the contact between the two opposite purlins. The matchboard was then placed on top of the timber structure.

To stiffen and strengthen the roof diaphragm (which originally was made only by a single layer of boards nailed to the joists), it was decided to adopt an intervention that was compatible with the original timber structure, by adding multilayer spruce plywood panels, which are lighter and easier to apply to an inclined plane in comparison to a reinforced concrete slab, although providing a significant stiffness increase. The intervention consisted in adding 3 layers of plywood, each 21 mm thick, glued with polyurethane glue and connected to the purlins by means of chemically anchored, 10 mm diameter threaded steel bars. After having drilled and cleaned the hole, a two-component epoxy mixture was inserted in the hole and then the bar was inserted and rotated to distribute the resin. Bars were placed at a constant spacing of 30 cm and penetrated into the purlins to connect the upper plank layers with the roof structure (Fig.3).

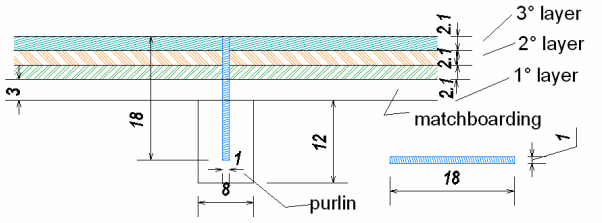

Figure 3. Scheme of the intervention on the roof diaphragm, consisting in the application of multilayer panels and chemically anchored steel connectors.

To improve the diaphragm behaviour of the roof, continuous steel plates (80 mm wide and 5 mm thick) were connected all along the perimeter to the roof, to favour the development of a strut and tie mechanism. The roof was then completed by adding plain roofing tiles nailed to the multilayer spruce

plywood panels.
Once the intervention on the roof was completed, also the intermediate floor was stiffened by means of a collaborating reinforced concrete topping, connected to the timber floor by means of shear dowels. As shown in Fig. 4, the intervention required the insertion of dowel elements (Turrini and Piazza, 1983), consisting of ϕ14 mm reinforcement bars bent at 90 degrees, epoxy-anchored in the joists through the existing plank layer, positioned at a spacing of 30 cm. The reinforcement of the topping consisted of a ϕ8 mm/150 mm steel welded mesh.

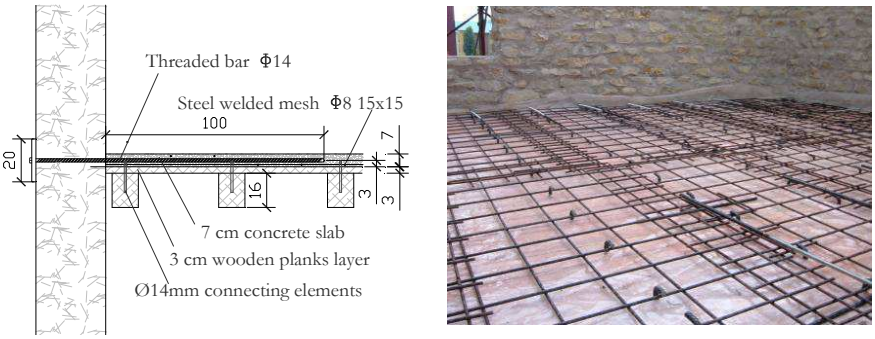

Figure 4. Details of the elements connecting the cast-in-place slab with the masonry wall (left) and layout of the reinforcement and the connecting elements within the collaborating slab (right).

The strengthening intervention was then completed by drilling through-holes in the peripheral walls to insert threaded ϕ14 mm bars, which would be anchored in the r.c. topping and bolted to steel plates positioned on the external surface of the walls. Such type of connection would exert a positive confinement of the masonry leaves at the floor level, preventing the separation of the external leaf. For several reasons, including construction tolerances, superposition of the mesh and intersection of the bars in the corners, it was necessary to cast a 7 cm thick slab to guarantee an adequate cover.

3. SHAKING TABLE TESTS

3.1 Instrumentation and acquisition

A set of accelerometers was installed on the structure to monitor a total of 48 different degrees of freedom. In addition to the accelerometers, displacement transducers were mounted to monitor table displacements and possible sliding of the roof elements on the top of the walls.

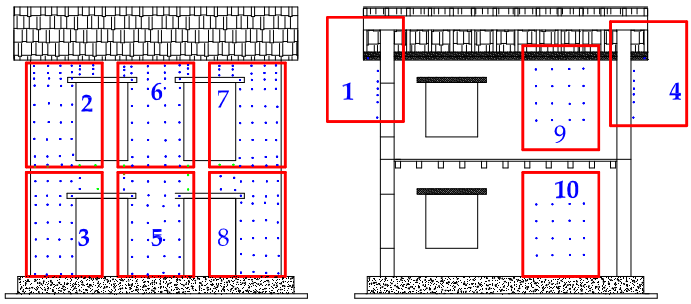

Figure 5. Position of markers for optical measurements of building 3: frames of cameras 2, 3, 5, 6, 7, 8, on West wall, 9-10 on East wall and 1 and 4 on North and South walls, respectively.

A system for optical measurement of absolute displacements by HD cameras was also used and a number of passive target markers were glued on the surface of the East and West walls in order to monitor their in-plane displacements (North-South direction). Markers were also fixed on North and South walls in order to monitor out-of-plane displacements (Fig. 5).

3.2 Shaking table testing procedure

3.2.1. Selection of accelerogram

As in the case of the two previously tested buildings (Magenes *et al.*, 2010a, Magenes *et al.* 2012), the third model has been subjected to a similar sequence of seismic excitation, by gradually increasing the intensity of the ground motion, scaling the reference input to selected values of nominal peak ground acceleration (PGA) up to a nominal PGA of 0.60g, where the specimen was close to collapse. The strong motion recorded during the 15th April 1979 Montenegro event at the Ulcinj-Hotel Albatros station was selected as seismic input to be applied. The choice of using the same signal for all the dynamic tests of the experimental program allowed monitoring the progressive damage to the structures and, at the same level of intensity of shaking, comparing the seismic response of structures that are typologically similar but with different strengthening interventions.

3.2.2. Dynamic tests

The strong motion imposed by the shaking table did not show a perfect agreement with the reference record because of the dynamic interaction between the shaking table and the structure to be tested. The discrepancy between the reference signal and the actual feedback from the shaking table is reflected by the differences between the nominal and actual PGA measured on the table, as reported in Tab. 3.2.

Table 3.2. Comparison of nominal and actual values of PGA and acceleration spectral ordinates of the response spectrum of the shaking table input in correspondence of the fundamental period of the structure T_1 ($Sa(T_1)$).

Test	Nominal PGA [g]	Actual PGA[g]
1	0.05	0.12
2	0.10	0.27
3	0.20	0.55
4	0.30	0.92
5	0.40	1.28
6	0.50	1.04
7	0.60	1.49
8	0.30 (AFTS*)	0.66

Test	T_1 [s]	Nominal Sa(T_1) [g]	Actual Sa(T_1) [g]
1	0.136	0.07	0.19
2	0.136	0.15	0.36
3	0.145	0.31	0.78
4	0.155	0.48	1.69
5	0.159	0.65	2.05
6	0.160	0.81	2.96
7	0.161	0.98	3.50
8	0.163	0.48	2.39

** AFTS: test simulating the occurrence of an aftershock*

As an example, in Fig. 6 the acceleration time history of the input signal of the test at nominal PGA of 0.60g is compared with the reference Montenegro acceleration record scaled at the same nominal PGA: the acceleration input is evidently distorted by amplification of the high frequency components of the signal.

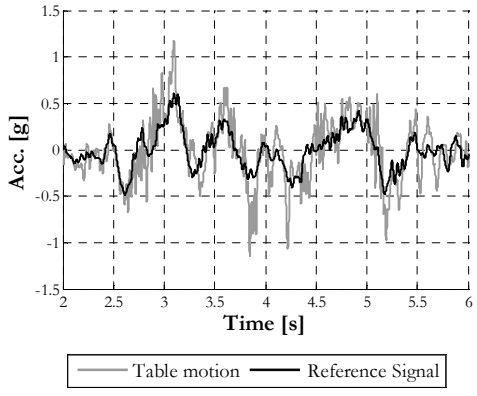

Figure 6. Acceleration time histories of the shaking table input during the test at nominal PGA of 0.60g.

As it can be seen in Fig. 7, where the acceleration spectra obtained for each dynamic test are compared with the spectrum of the theoretical input scaled at the same nominal PGA, the response spectra exhibit significant amplification of spectral ordinates in the range of periods below 0.50s, starting from

the test at nominal PGA of 0.30g. Furthermore, this amplification of the spectral ordinates occurs in the proximity of the fundamental period of the structure T_1, as evidenced both in Tab. 3.2 and in Fig. 6 by the dots indicating the spectral ordinates ($Sa(T_1)$) of the actual and theoretical input spectra. The period T_1 of the structure was identified by means of low-amplitude random excitation before each test run.

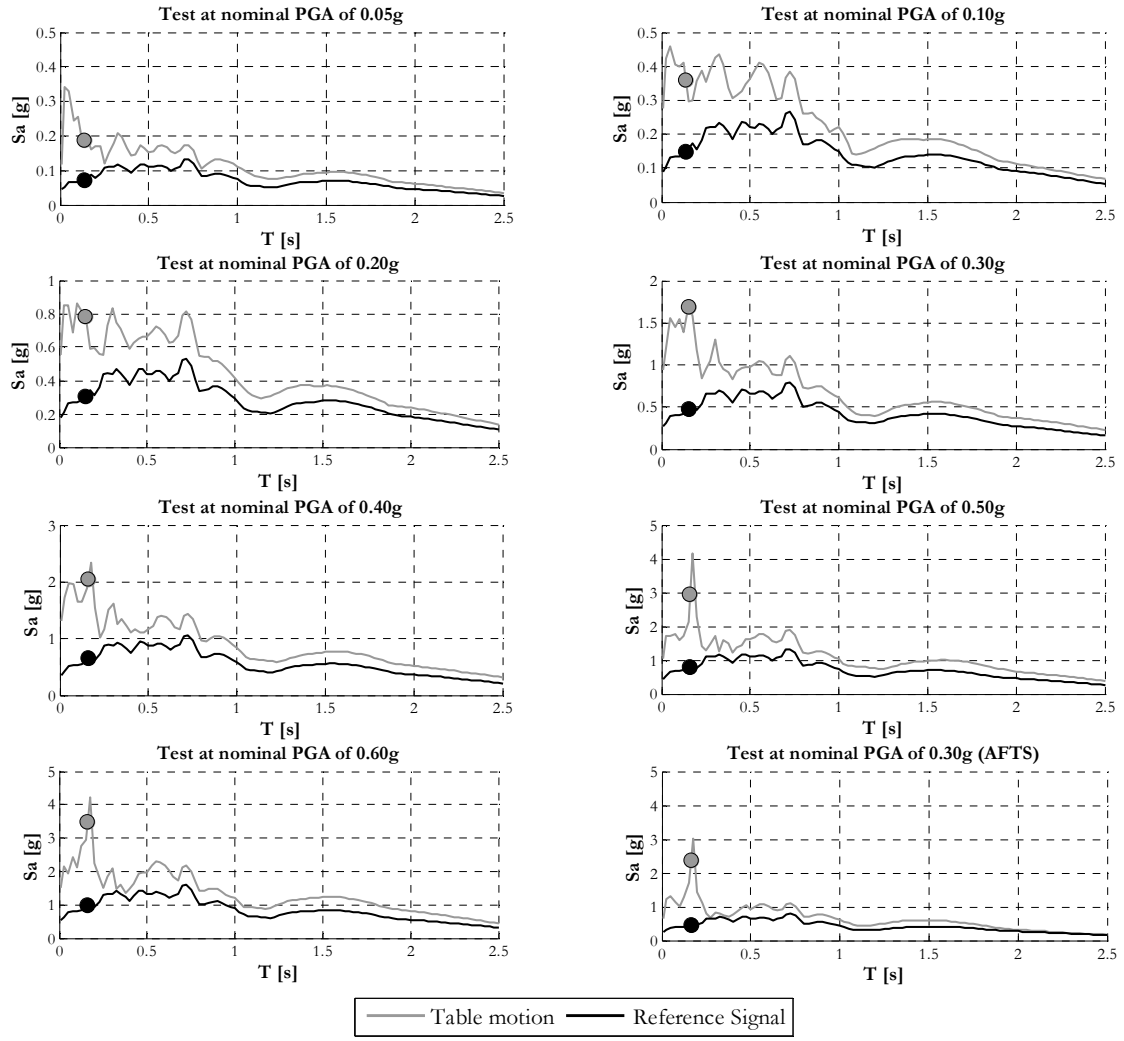

Figure 7. Comparison of the acceleration response spectra of the shaking table input for each test with the Montenegro record scaled at the same nominal PGA. The grey and black dots indicate the spectral ordinates at the fundamental period of the structure, for the actual and theoretical input spectra respectively.

The intensity of the table motion has been also evaluated through the computation of the Spectral Intensity and the Cumulative Absolute Velocity of the signals for each test performed, which are possible measures of the damage potential and of the cumulative effects of ground motion duration. The Spectral Intensity (I_{HM}) has been defined as the integral of the pseudo-velocity response spectrum (PSV) for periods in the range from 0.1 to 0.5s (rather than from 0.1 to 2.5s, as in the classical definition of Housner Intensity), as in Eqn. 4.1.

$$I_{HM} = \int_{0.1}^{0.5} PSV(T)dt \tag{4.1}$$

The Cumulative Absolute Velocity (CAV) is given by Eqn. 4.2, where $|a(t)|$ is the absolute value of the acceleration time series and t_{max} is the total duration of the shaking table input.

$$CAV = \int_0^{t_{max}} |a(t)| dt \tag{4.2}$$

As evident from Fig. 8, the third building was subjected to a much higher intensity of shaking in comparison to the reference Montenegro ground motion signal, with values that are almost 40% larger than the expected ones in terms of I_{HM} and approximately 50% larger in terms of *CAV*.

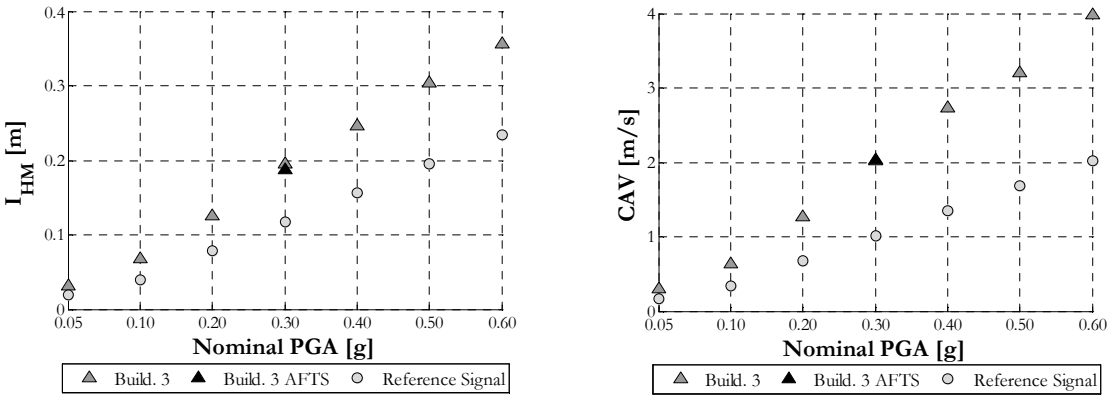

Figure 8. Plot of Spectral Intensity versus nominal PGA (left) and Cumulative Absolute Velocity versus nominal PGA (right)

4. OBSERVED DAMAGE PATTERNS AND COLLAPSE MECHANISMS

4.1 Observed damage during the transportation to the shaking table

The third prototype had already suffered some damage during transportation to the shaking table, due to some deformation of the foundation pad. The crack pattern was therefore similar to the one that would be present in case of differential settlements of the foundations.

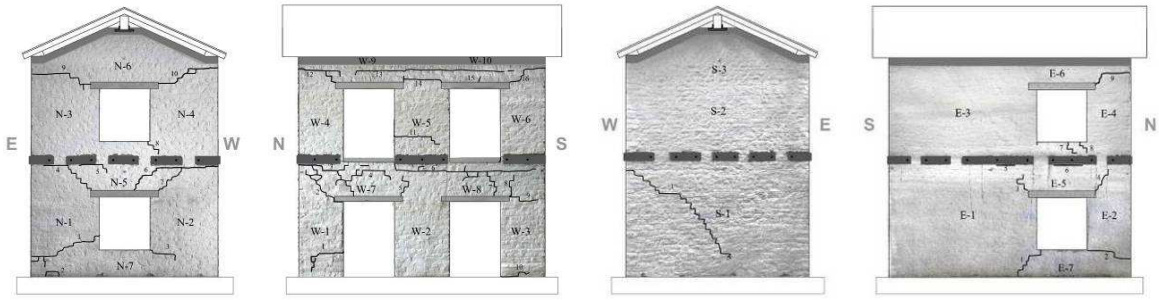

Figure 9. Crack pattern in the third building specimen after transportation to the shaking table. From left: North, West, South and East façade.

A detailed survey of the crack pattern was done (Fig. 9), detecting damage in the spandrels and cracks starting from the corners of the openings of all façades. The maximum measured crack width was 0.4mm. Although the pre-existing cracks have certainly affected to some extent the initial dynamic characteristics of the specimens, they have not affected the behaviour of the building at higher table motion intensities.

4.2 Observed damage after the test at a nominal PGA of 0.60g

The building was subjected to a sequence of seven shaking table tests, with increasing values of nominal PGA up to a maximum of 0.60g. The building experienced a substantial level of damage after the last test, in particular at the connection between the masonry walls and the first floor and at the interface between the stone masonry and the reinforced concrete ring beams (Fig. 10).

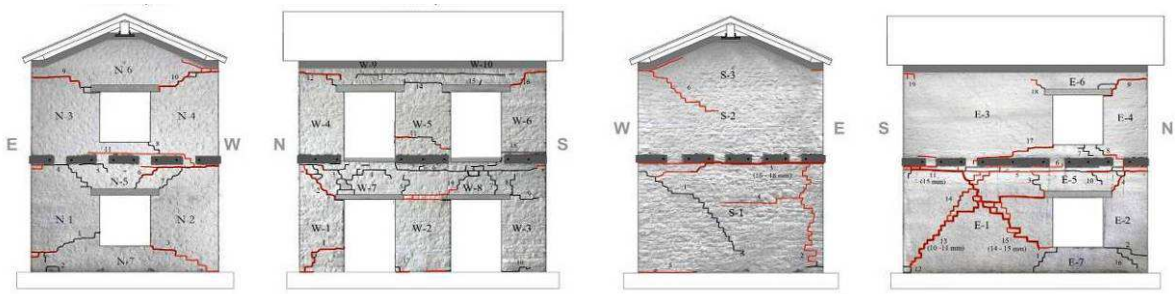

Figure 10. Crack pattern after the test at nominal PGA of 0.60g, from left: North, West, South and East façade.

As happened in the case of the second building (Magenes *et al*. 2012), the East façade exhibited a shear failure mechanism, with diagonal cracks opening in the pier at the first floor during the test at a nominal PGA of 0.50g. As evident from Fig. 11, where the instant of maximum opening of the cracks is shown, the diagonal cracks widened appreciably reaching up to 15mm width.

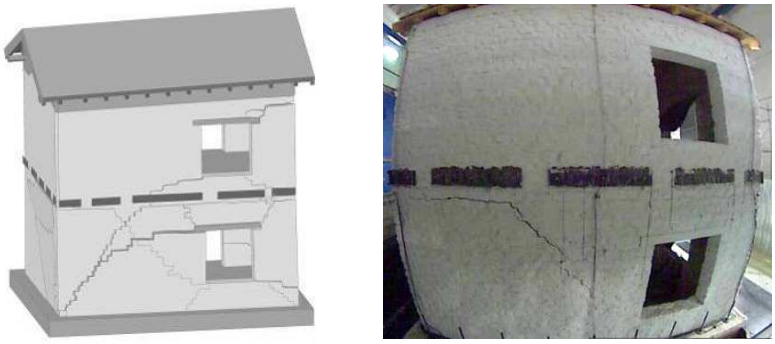

Figure 11. Test at a nominal PGA of 0.60g, East façade: shear failure mechanism (left) and instant of maximum opening of the diagonal cracks (right).

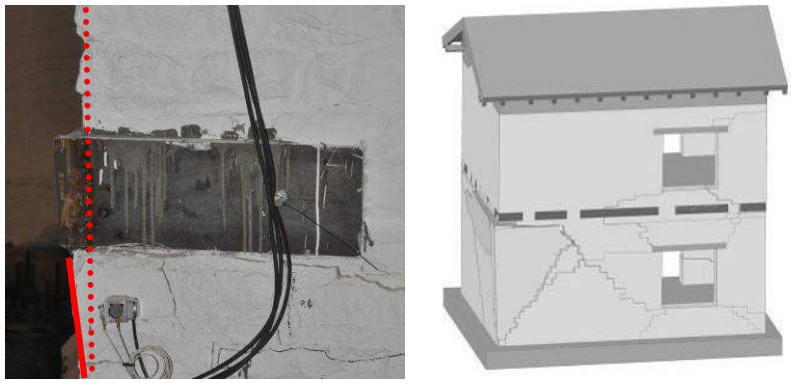

Figure 12. East façade, test at a nominal PGA of 0.60g: misalignment of the South-East corner (left) and corresponding overturning mechanism (right).

Given the severe shear cracking of the East wall it was decided not to increase further the shaking, to avoid total collapse of the specimen and damage to the testing facility. Besides the shear failure mechanism in the East façade, the crack pattern evidenced as well the incipient overturning of the

portion of masonry at the corner between the East and South walls. Lack of alignment between the lower and the upper piers of the two walls is clear in correspondence of the steel plates at the first floor level (Fig. 12, left).

The West façade exhibited in-plane rocking behaviour of the masonry piers at both levels, proved by the opening and widening of horizontal cracks at the base and top of each pier. The spandrel beams, already damaged during the transportation phase, sustained widening of the existing cracks, with the occurrence of additional shear diagonal cracks and decohesion of few stone blocks.

The presence of sufficiently rigid diaphragms and proper connections between walls and floor contributed to avoid the occurrence of local failure mechanisms, and in particular the overturning of portions of the transverse façades, as happened in the "unstrengthened" Building 1 (Magenes *et al*., 2010c). In particular, in Building 1 a local failure mode was activated which reached near-collapse conditions at a nominal PGA of 0.40g (corresponding to an actual table PGA of 0.63g and I_{HM} = 0.171m). The collapse mechanism involved the upper part of the North wall, which tended to overturn out-of-plane. On the contrary, in Building 3 it was possible to fully exploit the in-plane capacity of the longitudinal walls, attaining a near-collapse condition for a much higher intensity of shaking.

4.2 Observed damage after the test simulating an aftershock (nominal PGA of 0.30g)

After the test at 0.60g (nominal PGA), the prototype building was subjected to a last test at a nominal PGA of 0.30g, meant to simulate the effect of an aftershock on a damaged structure.

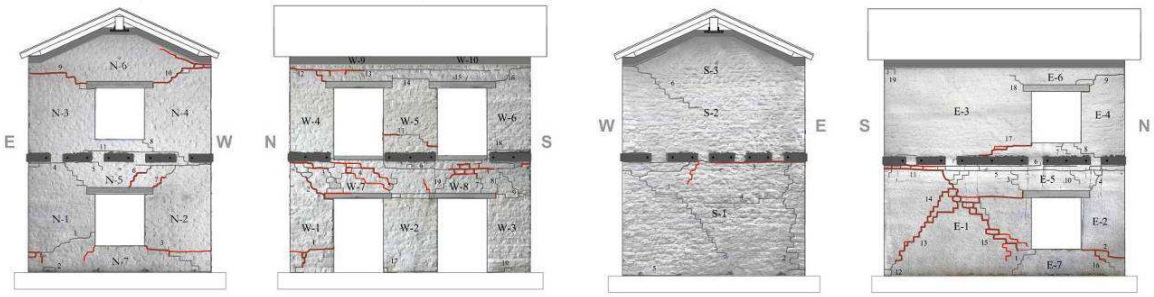

Figure 13. Crack pattern in the third specimen after the last test at a nominal PGA of 0.30g (AFTS), from left: North, West, South and East façade.

Figure 14. Decohesion of masonry blocks after the test with nominal PGA of 0.30g (aftershock): spandrel in the West façade (left), top of the base pier of the East wall (right).

Both longitudinal walls were characterised by a moderate widening and elongation of the existing cracks (Fig. 13), in particular in the longer pier of the East wall and at the interface between masonry walls and ring beam. Decohesion of masonry blocks also occurred in the masonry spandrels of the west façade as well as the interface between the piers and the steel plates in correspondence of the first floor of the East wall (Fig. 14). In general, it was felt that the building could have been able to withstand further shocks of similar intensity without the risk of total or partial collapses.

5. CONCLUSIONS

The shaking table tests provided meaningful results relevant to the seismic response of unreinforced stone masonry buildings and to the effectiveness of selected strengthening interventions. In the case of the third building tested in the experimental campaign performed at EUCENTRE, the strategy was to increase significantly the in-plane stiffness of the diaphragms, by means of a reinforced concrete slab cast on the existing first floor wood structure and the application of multilayer spruce plywood panels installed on the roof diaphragm. The latter solution is believed to be more compatible with the construction technologies of existing structures and lighter in weight, providing however comparable in-plane stiffness to that of a reinforced concrete slab.

The strengthening interventions applied on the Building 3 were designed to guarantee a box-type global response of the structure, preventing the occurrence of local out-of-plane damage mechanisms. Such objective was clearly obtained, since the building was able to withstand much stronger shaking than the original unstrengthened configuration (Magenes *et al*. 2010c), exploiting the in-plane capacity of the walls. However, from the first comparisons with the tests on a similar strengthened building (Magenes *et al*. 2012) maintaining moderately flexible diaphragms, it seems that the improvement on the seismic performance appears to be related more to the improvement of the floor-to-wall and roof-to-wall connections, rather than to a strong in-plane stiffening of the diaphragms. Further analysis and comparisons of the different tested buildings are currently ongoing.

ACKNOWLEDGEMENT

The research project was funded by the Italian Department of Civil Protection through the Executive Eucentre Project 2005-2008 and by the 2005-2008 Reluis Project, Line 1 and the 2010-2013 Reluis Project Task AT1-1.1. The authors would also like to acknowledge the support of the firms Tassullo Spa, Rothoblaas Srl and NV Bekaert SA in the construction of the building specimens. The EUCENTRE Lab, headed by prof. A. Pavese, and ITC service, as well as former students S. Pedolazzi, G. Andreotti, M. Da Paré and M. Acerbi provided valuable help. The suggestions of Prof. M. Piazza and Dr. R. Tomasi of the University of Trento and Prof. Modena of the University of Padua are gratefully acknowledged.

REFERENCES

Benedetti D., Carydis P., Pezzoli P. (1998) Shaking table test on 24 masonry buildings, *Earthquake engineering and Structural Dynamics*, Vol. 27, pp 67-90.

Dolce M., Ponzo F.C., Goretti A., Moroni C., Nigro D., Giordano F., De Canio G., Marnetto R. (2008) 3d dynamic tests on 2/3 scale masonry buildings upgraded with different systems, *Proc. 14th WCEE*, Beijing.

Graziotti, F., Magenes, G., Penna, A. (2012). Experimental cyclic behaviour of stone masonry spandrels. *Proc. of the 15th World Conference on Earthquake Engineering*. Lisbon.

Magenes G., Penna, A., Galasco A., Rota M. (2010a). Experimental characterisation of stone masonry mechanical properties. *Proc. 8th International Masonry Conference*, Dresden.

Magenes G., Galasco A., Penna A., Da Paré M. (2010b). In-plane cyclic shear tests of undressed double leaf stone masonry panels, *Proc. of the 14th European Conference on Earthquake Engineering*, Ohrid.

Magenes, G., Penna, A., and Galasco, A., (2010c). A full-scale shaking table test on a two storey stone masonry building. *Proc. of the 14th European Conference on Earthquake Engineering*. Ohrid.

Magenes G., Penna, A., Rota M. Galasco A., and Senaldi, I. (2012). Shaking table test of a full scale stone masonry building strengthened maintaining flexible floor and roof diaphragms *Proc. 8th International Conference on Structural Analysis of Historical Construction*, Wroclaw.

Mazzon N., Valluzzi M.R., Aoki T., Garbin E., De Canio G., Ranieri N., Modena C. (2009) Shaking table tests on two multi-leaf stone masonry buildings, *Proc. 11th Canadian Masonry Symposium*, Toronto.

NTC08 (2008) "Norme tecniche per le costruzioni," Ministero delle Infrastrutture e dei Trasporti, Decreto Ministeriale del 14 gennaio 2008, Supplemento ordinario alla G.U. n. 29 del 4 febbraio 2008 (in Italian)

Piazza, M., Baldessari, C. and Tomasi, R. (2008). The role of in-plane floor stiffness in the seismic behaviour of traditional buildings. *Proc. 14th World Conference on Earthquake Engineering,* Beijing

Tomazevic M. (1992) The influence of rigidity of floors on the seismic resistance of old masonry buildings: shaking-table tests of stone-masonry houses : summary report, ZRMK Report, 117p, Ljubljana.

Turrini, G. and Piazza, M. (1983) Una tecnica di recupero statico dei solai in legno, *Recuperare* **5**, 224-227. (in Italian)